

## Chapter 3

### The Finite Difference Time Domain (FDTD) Method

In this chapter, we provide a review of theoretical techniques of FDTD method employed in the current work. Our simulations are based on the well-known finite-difference time-domain (FDTD)[1] technique. The FDTD method is a rigorous solution to Maxwell's equations and does not have any approximations or theoretical restrictions. This method is widely used as a propagation solution technique in integrated optics, especially in situations where solutions obtained via the Plane Wave Expansion (PWE) [3,4] method cannot cope with the structure geometry or are not adequate solutions. FDTD is a direct solution of Maxwell's curl equations and therefore includes many more effects than a solution of the monochromatic wave equation. While most of these techniques are existing developed methods, the aim here is to provide a comprehensive picture of these methods.

#### 3.1. Discretizing Maxwell's equation in space and time

##### FDTD Method Introduction

Firstly introduced by Kane Yee in 1966 [1], the FDTD approach is based on a direct numerical solution of the time-dependent Maxwell's curl equations by using the Finite-Difference technique. This leads to a full-wave analysis for all wavelength information without any presumption to the material model and to the structure.

##### Maxwell's equation in three dimensions (3D)

The time-dependent Maxwell's equation for the homogeneous material with no electric or magnetic current sources can be expressed as:

$$\varepsilon \frac{\partial \vec{E}}{\partial t} + \sigma \vec{E} = \nabla \times \vec{H} \quad (3.1)$$

$$\mu_0 \frac{\partial \vec{H}}{\partial t} = -\nabla \times \vec{E} \quad (3.2)$$

Where  $\varepsilon = \varepsilon_r \varepsilon_0$  is the dielectric permittivity,  $\sigma$  is the conductivity, and  $\mu_0$  is the magnetic permeability of the vacuum. The refractive index is given by

$$n^2 = \varepsilon_r + \frac{\sigma}{j\omega\varepsilon_0}$$

We now write out the vector components of the above equations in Cartesian coordinates.

This yields the following system of six coupled scalar equations:

$$\mu_0 \frac{\partial \vec{H}_x}{\partial t} = \frac{\partial E_y}{\partial z} - \frac{\partial E_z}{\partial y} \quad 3.3a$$

$$\mu_0 \frac{\partial \vec{H}_y}{\partial t} = \frac{\partial E_z}{\partial x} - \frac{\partial E_x}{\partial z} \quad 3.3b$$

$$\mu_0 \frac{\partial \vec{H}_z}{\partial t} = \frac{\partial E_x}{\partial y} - \frac{\partial E_y}{\partial x} \quad 3.3c$$

$$\varepsilon \frac{\partial \vec{E}_x}{\partial t} + \sigma \vec{E}_x = \frac{\partial H_z}{\partial y} - \frac{\partial H_y}{\partial z} \quad 3.4a$$

$$\varepsilon \frac{\partial \vec{E}_y}{\partial t} + \sigma \vec{E}_y = \frac{\partial H_x}{\partial z} - \frac{\partial H_z}{\partial x} \quad 3.4b$$

$$\varepsilon \frac{\partial \vec{E}_z}{\partial t} + \sigma \vec{E}_z = \frac{\partial H_y}{\partial x} - \frac{\partial H_x}{\partial y} \quad 3.4c$$

### Maxwell's equations in two dimensions (2D)

In 2D simulation, we assume that the structure being modeled extends to infinity in the y-direction, and the photonic device is laid out in the x-z plane. The propagation is along z (or x). This assumption removes all the derivatives from Maxwell's equations and splits them into two (TE and TM) independent sets of equations.

#### TE mode Maxwell's equations in 2D

In the 2D TE cases, Maxwell's equations take the following form:

$$\mu_0 \frac{\partial H_x}{\partial t} = \frac{\partial E_y}{\partial z} \quad (3.5a)$$

$$\mu_0 \frac{\partial H_z}{\partial t} = \frac{\partial E_y}{\partial x} \quad (3.5b)$$

$$\varepsilon \frac{\partial E_y}{\partial t} + \sigma E_y = \frac{\partial H_x}{\partial z} - \frac{\partial H_z}{\partial x} \quad (3.5c)$$



In general,  $E_y$  is the major component in the simulation.

#### TM mode Maxwell's equations in 2D

In the 2D TM cases, Maxwell's equations take the following form:

$$\mu_0 \frac{\partial H_y}{\partial t} = \frac{\partial E_z}{\partial x} - \frac{\partial E_x}{\partial z} \quad (3.6a)$$

$$\varepsilon \frac{\partial H_y}{\partial t} + \sigma E_x = -\frac{\partial H_y}{\partial z} \quad (3.6b)$$

$$\mu_0 \frac{\partial H_x}{\partial t} + \sigma E_z = \frac{\partial H_y}{\partial x} \quad (3.6c)$$

In general,  $H_y$  is the major component in the simulation.

### Yee's Algorithm-FDTD equations

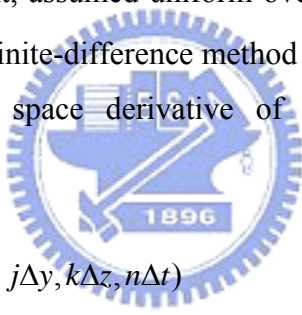
The Yee algorithm solves both the electric and magnetic fields in Maxwell's equations in time domain and space domain by using the finite-difference technique. It centers its  $E$  and  $H$  components in three-dimensional space so that every  $E$  component is surrounded by a circulating  $H$  component, and every  $H$  component is surrounded by a circulating  $E$  component.

### Finite Differences and notation

In general, a space point in the Cartesian system  $(x,y,z)$  in a uniform rectangular lattice can be denoted as:  $(i, j, k) = (i\Delta x, j\Delta y, k\Delta z)$  (3.7)

where  $\Delta x$ ,  $\Delta y$  and  $\Delta z$  are the space steps in the three directions. Following this, any function  $u(x,y,z,t)$  of space and time domain evaluated at a discrete point in the rectangular lattice can be denoted as:  $u(x, y, z, t) = u(i\Delta x, j\Delta y, k\Delta z, n\Delta t)u_{i,j,k}^n$  (3.8)

where  $\Delta t$  is the time increment, assumed uniform over the observation interval, and  $n$  is an integer. By using the centered finite-difference method that originally is derived from Taylor's series expansion, the partial space derivative of  $u$  in  $x$ -direction at the fixed time can be expressed as:  $t_n = n\Delta t$


$$\begin{aligned}\frac{\partial u(x, y, z, t)}{\partial x} &= \frac{\partial}{\partial x} u(i\Delta x, j\Delta y, k\Delta z, n\Delta t) \\ &= \frac{u_{i+1/2,j,k}^n - u_{i-1/2,j,k}^n}{\Delta x} + O[(\Delta x)]^2\end{aligned}\quad (3.9)$$

### Three Dimensional FDTD equations

In a 3D simulation, the simulation domain is a cubic box, the space steps are  $\Delta x, \Delta y$ , and  $\Delta z$  in  $x, y$ , and  $z$  directions respectively. Each field component is presented by a 3D array— $E_x(i,j,k)$ ,  $E_y(i,j,k)$ ,  $E_z(i,j,k)$ ,  $H_x(i,j,k)$ ,  $H_y(i,j,k)$ ,  $H_z(i,j,k)$ . The field component positions in Yee's Cell are shown in Figure 3.1. This placement and the notation cause the  $E$  and  $H$  components to be interleaved at intervals of in space and for the purpose of implementing a leapfrog algorithm.

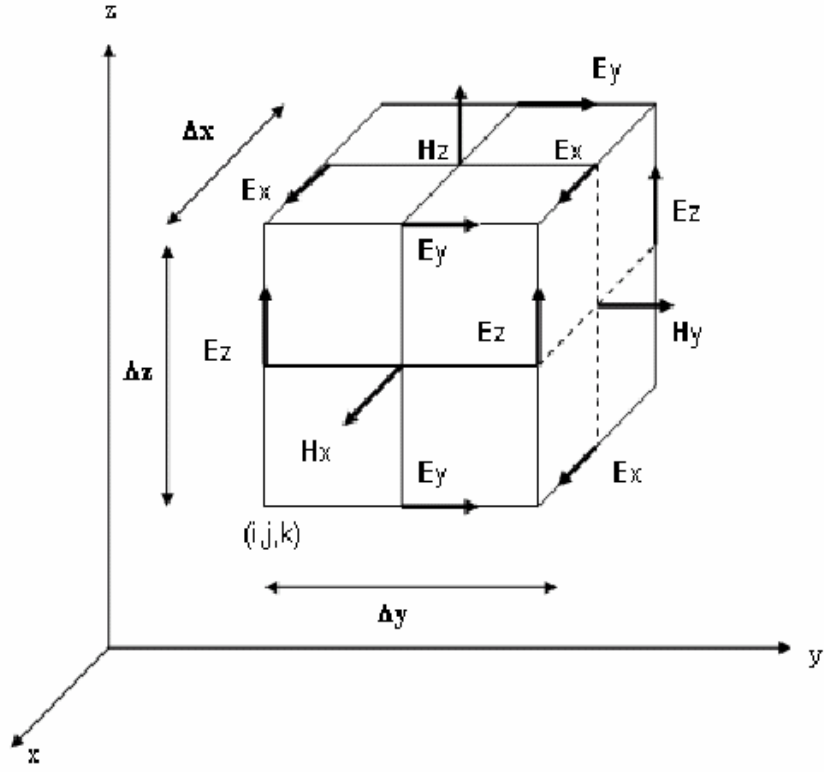


Figure 3.1 In a Yee cell dimension  $\Delta_x$ ,  $\Delta_y$ ,  $\Delta_z$ , note how the H field is computed at points shifted one-half grid spacing from the E field grid points [1].

Now we can apply the above finite-difference ideas, notation and field displacement to achieve a numerical approximation of Maxwell's equation (3-3 - 3-4). The FDTD equation can be written as:

$$H_{x,i,j-1/2,k-1/2}^{n+1/2} = H_{x,i,j-1/2,k-1/2}^{n-1/2} + \frac{\Delta t}{\mu_0 \Delta z} (E_{y,i,j-1/2,k}^n - E_{y,i,j-1/2,k-1}^n) - \frac{\Delta t}{\mu_0 \Delta z} (E_{z,i,j,k-1/2}^n - E_{z,i,j-1,k-1/2}^n) \quad (3.11a)$$

$$H_{y,i,j-1/2,k-1/2}^{n+1/2} = H_{y,i,j-1/2,k-1/2}^{n-1/2} + \frac{\Delta t}{\mu_0 \Delta x} (E_{z,i,j,k-1/2}^n - E_{z,i,j-1,k-1/2}^n) - \frac{\Delta t}{\mu_0 \Delta z} (E_{x,i-1/2,j,k}^n - E_{x,i-1/2,j,k-1}^n) \quad (3.11b)$$

$$H_{z,i-1/2,j-1/2,k}^{n+1/2} = H_{z,i-1/2,j-1/2,k}^{n-1/2} + \frac{\Delta t}{\mu_0 \Delta y} (E_{x,i-1/2,j,k}^n - E_{x,i-1/2,j-1,k}^n) - \frac{\Delta t}{\mu_0 \Delta x} (E_{y,i,j-1/2,k}^n - E_{y,i-1,j-1/2,k}^n) \quad (3.11c)$$

$$E_{x,i-1/2,j,k}^{n+1} = \frac{2\varepsilon - \sigma\Delta t}{2\varepsilon + \sigma\Delta t} E_{x-1/2,i,j,k}^n + \frac{2\Delta t}{(2\varepsilon + \sigma\Delta t)\Delta t} (H_{z,i-1/2,j+1/2,k}^{n+1/2} - H_{z,i-1/2,j-1/2,k}^{n+1/2}) - \frac{2\Delta t}{(2\varepsilon + \sigma\Delta t)\Delta t} (H_{y,i-1/2,j,k+1/2}^{n+1/2} - H_{y,i-1/2,j,k-1/2}^{n+1/2}) \quad (3.12a)$$

$$E_{y,i,j-1,k}^{n+1} = \frac{2\varepsilon - \sigma\Delta t}{2\varepsilon + \sigma\Delta t} E_{y,i,j-1/2,k}^n + \frac{2\Delta t}{(2\varepsilon + \sigma\Delta t)\Delta t} (H_{x,i,j-1/2,k+1/2}^{n+1/2} - H_{x,i,j-1/2,k-1/2}^{n+1/2}) - \frac{2\Delta t}{(2\varepsilon + \sigma\Delta t)\Delta t} (H_{z,i+1/2,j-1/2,k}^{n+1/2} - H_{z,i-1/2,j-1/2,k}^{n+1/2}) \quad (3.12b)$$

$$E_{z,i,j,k-1/2}^{n+1} = \frac{2\varepsilon - \sigma\Delta t}{2\varepsilon + \sigma\Delta t} E_{z,i,j,k-1/2}^n + \frac{2\Delta t}{(2\varepsilon + \sigma\Delta t)\Delta t} (H_{y,i,j-1/2,k+1/2}^{n+1/2} - H_{y,i,j-1/2,k-1/2}^{n+1/2}) - \frac{2\Delta t}{(2\varepsilon + \sigma\Delta t)\Delta t} (H_{x,i,j+1/2,k-1/2}^{n+1/2} - H_{x,i,j-1/2,k-1/2}^{n+1/2}) \quad (3.12c)$$

## 2D TE Wave FDTD equation

The 2D computational domain is shown in Figure 3.2. The space steps in the x and z directions are  $\Delta x$  and  $\Delta z$ , respectively. Each mesh point is associated with a specific type of material and contains information about its properties, such as refractive index and dispersion parameters

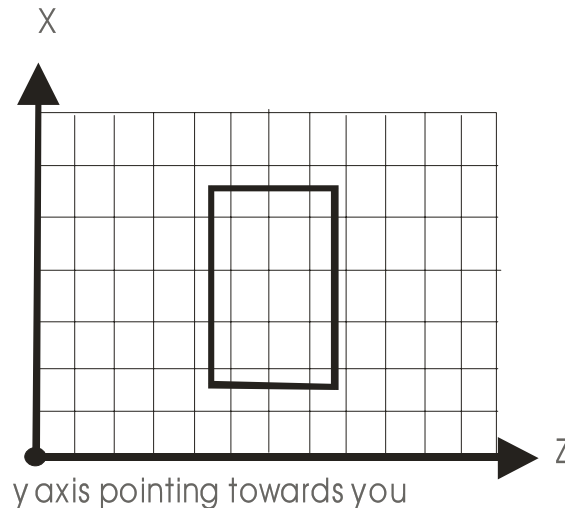


Figure 3.2 Numerical representation of the 2D computational domain

In the 2D TE simulation, Each field is represented by a 2D array— $E_y(i,k)$ ,  $H_x(i,k)$  and  $H_z(i,k)$ —corresponding to the 2D mesh grid shown in Figure 3.2. The indices  $i$  and  $k$  account for the number of space steps in the X and Z directions, respectively. The location of the fields in the mesh is shown in Figure 3.3.

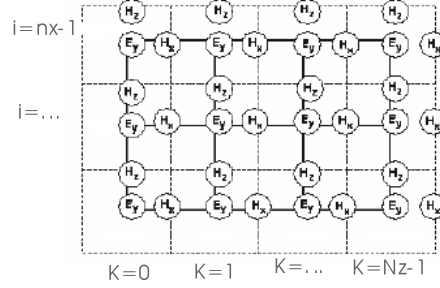


Figure 3.3 Location of the TE fields in the computational domain

$$H_{x,i,k+1/2}^{n+1/2} = H_{x,i,k+1/2}^{n-1/2} + \frac{\Delta t}{\mu_0 \Delta z} (E_{y,i,k+1}^n - E_{y,i,k-1}^n) \quad (3.13a)$$

$$H_{z,i+1/2,k}^{n+1/2} = H_{z,i+1/2,k}^{n-1/2} + \frac{\Delta t}{\mu_0 \Delta x} (E_{y,i+1,k}^n - E_{y,i,k}^n) \quad (3.13b)$$

$$E_{y,i,k}^{n+1} = \frac{2\varepsilon - \sigma\Delta t}{2\varepsilon + \sigma\Delta t} E_{y,i,k}^n + \frac{2\Delta t}{(2\varepsilon + \sigma\Delta t)} (H_{x,i,k+1/2}^{n+1/2} - H_{x,i,k-1/2}^{n+1/2}) - \frac{2\Delta t}{(2\varepsilon + \sigma\Delta t)} (H_{z,i+1/2,k}^{n+1/2} - H_{z,i-1/2,k}^{n+1/2}) \quad (3.13c)$$

## 2D TM wave FDTD equation

In the 2D TM simulation, Each field is represented by a 2D array— $H_y(i,k)$ ,  $E_x(i,k)$  and  $E_z(i,k)$ —corresponding to the 2D mesh grid given in Figure 3.2. The location of the TM fields in the computational domain follows the same philosophy and is shown in Figure 3.4.

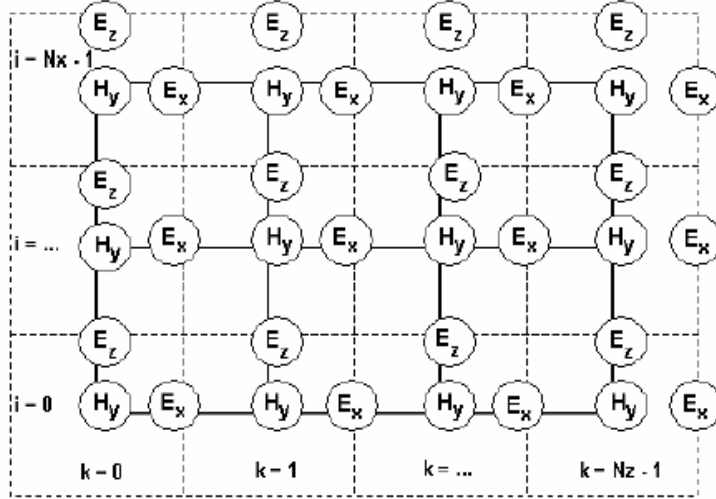


Figure 3.4 Location of the TM fields in the computational

$$H_{y,i,k}^{n+1/2} = H_{y,i,k}^{n-1/2} + \frac{\Delta t}{\mu_0 \Delta x} (E_{z,i+1/2,k}^n - E_{z,i-1/2,k}^n) - \frac{\Delta t}{\mu_0 \Delta z} (E_{x,i,k+1}^n - E_{x,i,k-1/2}^n) \quad (3.14a)$$

$$E_{x,i+1/2,k}^{n+1} = \frac{2\varepsilon - \sigma\Delta t}{2\varepsilon + \sigma\Delta t} E_{x,i,k}^n - \frac{2\Delta t}{(2\varepsilon + \sigma\Delta t)\Delta x} (H_{y,i,k+1/2}^{n+1/2} - H_{y,i,k-1/2}^{n+1/2}) \quad (3.14b)$$

$$E_{z,i,k+1/2}^{n+1} = \frac{2\varepsilon - \sigma\Delta t}{2\varepsilon + \sigma\Delta t} E_{z,i,k+1/2}^n + \frac{2\Delta t}{(2\varepsilon + \sigma\Delta t)\Delta x} (H_{y,i+1/2,k}^{n+1/2} - H_{y,i-1/2,k}^{n+1/2}) \quad (3.14c)$$

### Space step and time step

The fundamental constraint of the FDTD method is the step size both for the space and time. Space and time steps relate to the accuracy, numerical dispersion, and stability of the FDTD method. Many references and books discuss these problems [4,5]. In general, to ensure that the results are accurate and have a low numerical dispersive, the mesh size is often quoted as "10 cells per wavelength", meaning that the side of each cell should be  $\lambda / 10$  or less at the highest frequency (shortest wavelength). Note that FDTD method is volumetric computational method, so that if some portion of the computational space is filled with penetrable material, we must use the wavelength in the material to determine the maximum cell size. The following equation is for the suggested mesh size

$$\text{minimum}(\Delta x, \Delta y, \Delta z) \leq \frac{\lambda_{\min}}{10n_{\max}} \quad (3.15)$$

where  $n_{\max}$  is the maximum refractive index value in the computational domain. Once the cell size is determined, the maximum size for the time step immediately follows the Courant-Friedrichs-Lewy (CFL) condition. For a 3D FDTD simulation, the CFL condition is:

$$\Delta t \leq \frac{1}{v \sqrt{\frac{1}{(\Delta x)^2} + \frac{1}{(\Delta y)^2} + \frac{1}{(\Delta z)^2}}} \quad (3.16)$$

where  $v$  is the speed of the light in medium.

For a 2D simulation, the above CFL condition can be simplified as:

$$\Delta t \leq \frac{1}{v \sqrt{\frac{1}{(\Delta x)^2} + \frac{1}{(\Delta y)^2}}} \quad (3.17)$$

### **FDTD Boundary condition**

The boundary conditions [8,9] at the spatial edges of the computational domain must be carefully considered. Many simulations employ an absorbing boundary condition that eliminates any outward propagating energy that impinges on the domain boundaries. One of the most effective is the perfectly matched layer (PML) [8], in which both electric and magnetic conductivities are introduced in such a way that the wave impedance remains constant, absorbing the energy without inducing reflections.

### **Periodic boundary conditions (PBC)**

Periodic boundary conditions (PBC) [9] are also important because of their applicability to PBG structures. There are a number of variations on the PBC, but they all share the same common thread: the boundary condition is chosen such that the simulation is equivalent to an infinite structure composed of the basic computational domain repeated endlessly in all dimensions. PBCs are most often employed when analyzing periodic structures. Periodic boundary conditions are quite useful when working with periodic structure types. A periodic boundary stipulates that any field which leaves the boundary on one side of the domain should reenter the domain on the opposite side. This can be expressed mathematically as  $E(x_i) = E(x_i + \Delta) \exp(k_i x_i)$  where the structure is assumed to be periodic along the coordinate with period  $\Delta$  and a phase difference  $k_i$ . The period is defined by the length of the domain



along the specified coordinate  $x_i$ . Periodic boundaries can only be applied to any combination of the three coordinates, but cannot be applied to each boundary individually.

### **Symmetric**

Symmetric boundary conditions assume that the field is symmetric about one or more planes of reflection, and are also known as “even” boundary conditions. This is useful when both the structure and the simulated fields have symmetry about one or more planes of reflection. This can be expressed mathematically as  $\mathbf{E}(x_i) = \mathbf{E}(-x_i)$ , where  $x_i$  is the specified coordinate about which the field is to be assumed symmetric. The position of the reflection plane is given by the domain definition. Symmetric boundary conditions can be applied to any combination of the three coordinates as well as each of the six boundaries individually.

### **Anti-Symmetric**

Anti-Symmetric boundary conditions assume that the field is anti-symmetric about one or more planes of reflection, and are also known as “odd” boundary conditions. The field is therefore set to 0 at the boundary, and the fields on both sides of the boundary are assumed to be of opposite sign. This can be useful for symmetric structures which support an antisymmetric field, for instance anti-symmetric mode  $\mathbf{E}(x_i) = -\mathbf{E}(-x_i)$ , where  $x_i$  is the specified coordinate about which the field is to be assumed anti-symmetric. The position of the reflection plane is given by the domain definition. Anti-symmetric boundary conditions can be applied to any combination of the three coordinates as well as each of the six boundaries individually.

### **Input Wave**

The FDTD numerical scheme yields the solution of an initial value problems, The algorithm requires the initial field excitation that will be propagated through the computational domain. The Input Wave must contain four kinds of the information: (1) Input wave propagation direction (2) Input wave formation in time domain (3) Input wave profile in transverse plane (4) Polarization. Total-Field/Scattered-Field (TF/SF) results from attempts to realize a wave propagation in a desired direction. The computational domain is separated into two sub-regions—the total field region and the reflected field region. The plane separating these regions is called the incident field (input plane) (see Figure 3.5).

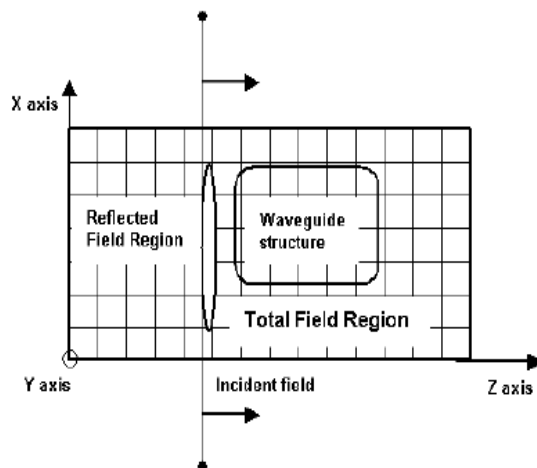


Figure 3.5 Total/Reflected field formulation

In the Total Field Region, the waveguide structures of interest are designed. The interaction between the incident field and the waveguide structure take place in this region. This is why the Total Field Region contains information for both the incident and scattered (reflected) waves. In the Reflected Field Region, the geometry is uniform and the propagating waves are presented by the fields reflected from the Total Field Region. There are no objects in this region, and the signal will not be reflected back to the total field region. Continuous wave (CW) or pulsed excitations can be used. You can consider the incident field as being generated by a flashlight located on the incidence plane facing the +Z direction. Before starting the simulation, the flashlight is turned off and the field values in the whole computational domain are equal to zero. The flashlight is switched on at  $t = 0$  and illuminates only the Total Field Region. If the excitation scheme is perfect, there should not be any light detected by an observer located in the Reflected Field Region, unless there are some obstacles which would generate the reflections. The incident wave can be generated by specifying the exact field distribution on the incident plane at each time interval. The TF/SF requires the special treatment for FDTD equation in the Input plane.

### **Input Wave formation in time domain**

Two kinds of time domain input wave formations can be simulated in the FDTD. One is for the single wavelength simulation-the Continuous Wave (CW) input. The other is for the wide band simulation-the Gaussian Modulated Continuous Wave (GMCW). In general, it is called Pulsed Input.

## CW Excitation

In CW excitation, the time dependence of the incident field is a single frequency sinusoidal function. For example the incident  $E_y$  field has the following form:

$$E_y^{inc}(x, z_{inc}) = AT(t)F(x, z_{inc})\sin(\omega t + \theta_i) \quad (3.18)$$

where  $A$  is the field amplitude,  $AF(x, z_{inc})$  is the transverse field distribution at the incident plane location  $z_{inc}$ . The initial phase offset  $\theta_i$  is the phase difference between points in the incidence plane. This offset can be adjusted to define the direction of the incident field.  $\omega = (2\pi/\lambda)c$  is the frequency of the input wave. In the CW case the optical wave analog propagates until it reaches the stationary state everywhere in the computational window.

## Gaussian Modulated Continuous Wave (GMCW) Excitation (Pulsed Excitation)

For pulsed excitations the incident field has the form:

$$E_y^{inc}(x, z_{inc}) = AF(X, Z_{inc})\sin(\omega t + \theta_i) \quad (3.19)$$

$$E_y^{inc}(x, z_{inc}) = AT(t)F(x, z_{inc})\sin(\omega t + \theta_i) \quad (3.20)$$

where

$$T(t) = \exp\left[-\frac{1}{2}\left(\frac{t-t_{off}}{t_0}\right)^2\right] \quad (3.21)$$

is the pulse envelope function,  $t_{off}$  is the time offset and  $t_0$  is the pulse width parameter. For pulsed excitations the time stepping continues until the desired late-time pulse response is observed at the field points of interest.

## Gaussian Transverse excitation

For Gaussian Transverse excitation, the transverse field has a Gaussian profile that can be calculated from the following equation:

$$E(x, y) = \exp\left[-\frac{1}{2}\left(\frac{x-x_0}{X}\right)^2\right]\exp\left[-\frac{1}{2}\left(\frac{y-y_0}{Y}\right)^2\right] \quad (3.22)$$

Where  $(x_0, y_0)$  is the center point where the Gaussian beam has the peak value.  $X$  and  $Y$  are the half widths.

### Material Model [6,7]

One of the main advantages of the FDTD approach is the lack of approximations for the propagating field-light is modeled in its full richness and complexity. The other significant advantage is the great variety of materials that can be consistently modeled within the FDTD context. Here, we make a brief review of some of the main material properties that can be handled.

### Lossy dielectrics

Before proceeding with a more detailed description, it should be emphasized that the fact that in the time domain all the fields ( $H_x, E_y, H_z$ ) are real quantities. Thus, accounting for loss is possible only through a non-zero conductivity  $\sigma$  of the medium:

$$\nabla \times \vec{H} = \varepsilon_0 \varepsilon \frac{\partial \vec{E}}{\partial t} + \sigma \vec{E} = i\omega \varepsilon_0 \left( \varepsilon_r - i \frac{\sigma}{\omega \varepsilon_0} \right) \vec{E} = i\omega \varepsilon_0 \varepsilon_{\text{eff}} \vec{E} \quad (2.23)$$

Here we have assumed that  $\vec{E} \propto e^{i\omega t}$  and  $\frac{\partial}{\partial t} \rightarrow i\omega$  corresponds to time-to-frequency domain Fourier transform. The real and imaginary part of the permittivity can be expressed through the real and imaginary part of the *Imaginary* refractive index:

$$\varepsilon_e^{\text{Re}} = n^2 - \kappa^2, \varepsilon_r^{\text{Im}} = 2n\kappa, \kappa = -2\varepsilon_0 \omega n / \sigma \quad (3.24)$$

This makes the refractive index approach and the conductivity approach equivalent.

### Sellmeier equation model

In the Sellmeier equation model, the material constant refractive index for the user specified wavelength is calculated by the Sellmeier equation:

$$n^2 = A_0 + \sum_{m=1}^M \frac{A_m \lambda^2}{\lambda^2 - i\Gamma_m - \lambda_m^2} \quad (3.25)$$

Where  $A$  is the Strength,  $\lambda$  is the resonant wavelength,  $\Gamma_m$  the damping coefficient, and

$\lambda_m$  is the working wavelength. Note that there are two applications for the Sellmeier equation model in the FDTD. One is used to calculate the constant refractive index for a material. It is the constant refractive index coupled into the Maxwell's equation, and not the Sellmeier equation coupled into Maxwell's equation, so in such a simulation, the material still does not have the dispersive properties. The second application for Sellmeier equation is to transfer the Sellmeier model to Lorentz model that will be coupled into Maxwell's equation. In such a simulation, the material will have the dispersive.

### Lorentz Dispersion material

By Lorentz dispersion materials, we mean materials for which the frequency dependence of the dielectric permittivity can be described by a sum of multiple resonance Lorentzian functions:

$$\varepsilon_r(\omega) = \varepsilon_\infty + \sum_{m=1}^N \frac{\chi_0 G_m \omega_m^2}{\omega_m^2 + i\Gamma_m \omega - \omega^2}, \sum_{m=1}^N G_m = 1 \quad (3.26)$$

where

$\omega_{0m}$  are the resonant frequencies

$G_m$  is related to the oscillator strengths

$\Gamma_m$  is the damping coefficient

$\varepsilon_\infty$  is the permittivity at infinite frequency

$\chi_0 = \varepsilon_s - \varepsilon_\infty$  is the permittivity at  $\omega = 0$

In the lossless case, Equation 3.26 is directly related to the Sellmeier equation which in the three resonances can be presented as:

$$n^2 = \varepsilon_\infty + \frac{A_1 \lambda^2}{\lambda^2 - \lambda_1^2} + \frac{A_2 \lambda^2}{\lambda^2 - \lambda_2^2} + \frac{A_3 \lambda_2}{\lambda^2 - \lambda_3^2}, A_m = \chi_0 G_m, (m = 1, 2, 3) \quad (3.27)$$

In the lossy case, the Sellmeier equation can be written in a generalized form, accounting for a non-zero damping coefficient  $\Gamma_m$ , as well as for anisotropy in the dispersion properties:

$$n^2(\omega) = \varepsilon_\infty + \frac{A_1 \lambda^2}{\lambda^2 + i\Gamma_{\lambda_1} \lambda - \lambda_1^2} + \frac{A_2 \lambda^2}{\lambda^2 + i\Gamma_{\lambda_2} \lambda - \lambda_2^2} + \frac{A_3 \lambda_2}{\lambda^2 + i\Gamma_{\lambda_3} \lambda - \lambda_3^2} \quad (3.28)$$

There are different ways to implement Equation 3.26 into the FDTD formalism. Here we consider the so-called polarization equation approach in the single resonance case. It uses the

dielectric susceptibility function:

$$\chi(\omega) = \frac{\chi_0 \omega_0^2}{\omega_0^2 + i\Gamma\omega - \omega^2} \quad (3.29)$$

and the relation between the polarization and the electric field. Taking the Fourier transform of the last equation leads to the following differential equation:

$$\frac{\partial^2 P_y}{\partial t^2} + \Gamma \frac{\partial P_y}{\partial t} + \omega_0^2 P_y = \varepsilon_0 \chi_0 \omega_0^2 E_y \quad (3.30)$$

### Drude model material

Drude model is another dispersion effect. In most cases, it simulates the noble metal or the surface plasma. Materials with Drude dispersion are optically linear materials for which the frequency dependence of the dielectric permittivity can be described by the Drude Dispersion relation:

$$\varepsilon_r(\omega) = \varepsilon_{\infty} + \frac{\omega_p^2}{i\Gamma\omega - \omega_2} \quad (3.31)$$



where  $\omega_p$  is the plasma frequency and  $\Gamma$  is the damping rate. The above equation only describes the dispersion relation in frequency domain. Because FDTD is a time domain method, the Drude model must be transferred to the time domain and solved in time domain. For Drude material, the corresponding Maxwell's equations are:

$$\begin{aligned} \nabla \times \vec{H} &= \varepsilon_{\infty} \frac{\partial \vec{E}}{\partial t} + \vec{J} \\ \nabla \times \vec{E} &= -\mu_0 \frac{\partial \vec{H}}{\partial t} \\ \frac{\partial \vec{J}}{\partial t} + \Gamma \vec{J} &= \varepsilon_0 \omega_p^2 \vec{E} \end{aligned} \quad (3.32)$$

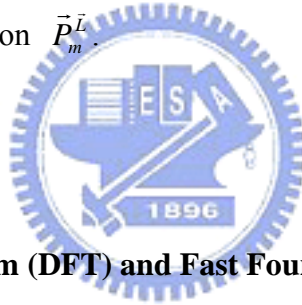
The FDTD scheme for Drude material can be derived from the above equations by using the finite-difference technique.

### Dispersive Nonlinear materials

In general, the nonlinear behavior is due to the dependence of the polarization  $P(t)$  on the applied electric field,  $E(t)$ . Assuming an isotropic dispersive material, Maxwell's equations are:

$$\begin{aligned}
 \mu_0 \frac{\partial \vec{H}}{\partial t} &= -\nabla \times \vec{E} \\
 \frac{\partial \vec{D}}{\partial t} &= \nabla \times \vec{H} \\
 \vec{D} &= \vec{P}^L + \vec{P}^{NL} + \sum_{m=1} \vec{P}_m^D \\
 \frac{\partial^2 \vec{P}_m^L}{\partial t^2} + \Gamma_m \frac{\partial \vec{P}_m^L}{\partial t} + \omega_m^2 \vec{P}_m^L &= \varepsilon_0 \chi_0 G_m \omega_m^2 \vec{E}
 \end{aligned} \tag{3.33}$$

Where  $\vec{P}^L$  represents the linear polarization, in general  $\vec{P}^L = \varepsilon_L \varepsilon_0 \vec{E}$ ,  $\vec{P}_m^D$  is the dispersive polarization which is controlled by Lorentz model in Equation 3.33 and denotes the nonlinear polarization  $\vec{P}_m^{NL}$ .



### Post Data Analysis

#### Discretized Fourier Transform (DFT) and Fast Fourier Transform (FFT)

FDTD is time domain simulation method. It can obtain all the desired spectral responses through a one-time simulation. To obtain the spectral response, you must use the DFT and FFT and Analysis.

#### Discretized Fourier Transform obtains a single wavelength response from a time series.

where  $s(n)$  is the time domain response,  $N$  is the time steps number, and  $\omega$  is the angle frequency. When DFT is running in the simulation, it obtains the frequency domain response for the center wavelength only, while DFT for the observation point, area, and line provides the spectral response for a series of user-specified wavelengths. Fast Fourier Transform uses the traditional fast Fourier transform scheme to obtain a spectral response from the zero frequency to the cutoff frequency. The frequency domain sampling step is  $\Delta\omega = \frac{2\pi}{N\Delta t}$ . In general, the sampling frequency step for FFT is comparable to the interested wavelength due to the fact that FDTD required time step is very small. So the FFT results may have larger errors than that of the DFT results. But FFT is much faster than DFT.

## Power calculation and Poynting vector

For the z-direction propagation wave. The total power in the x-y plane can be divided into two power values: x-direction polarized z-direction propagation power ( $P_{z-x}$ ) and y-direction polarized z-direction propagation power ( $P_{z-y}$ ). The corresponding formulas are:

$$\begin{aligned}
 x - \text{polarization power } P_{z-x} &= \text{Re}\left(\frac{1}{2} \iint_s E_x H_y^* dx dy\right) \\
 y - \text{polarization power } P_{z-y} &= -\text{Re}\left(\frac{1}{2} \iint_s E_y H_x^* dx dy\right) \\
 \text{Total power } P_z &= P_{z-x} + P_{z-y} = \text{Re}\left(\frac{1}{2} \iint_s E_x H_y^* dx dy\right) - \text{Re}\left(\frac{1}{2} \iint_s E_y H_x^* dx dy\right)
 \end{aligned} \tag{3.34}$$

Where the cap dot means the complex value which comes from the DFT calculation, and the superscript star means the complex conjugate value. The z-direction Poynting for a point  $(i,j)$  in x-y plane is

$$S_{z,i,j} = \frac{1}{2} E_{x,i,j} H_{y,i,j}^* - \frac{1}{2} E_{y,i,j} H_{x,i,j}^* \tag{3.35}$$

Poynting vector is a complex value. In FDTD, only the amplitude is shown.

## 3.2 Advantages versus drawbacks of the FDTD method

The FDTD approach has several key advantages over all of the preceding methods, as well as several drawbacks. The leapfrog time stepping mechanism used is fully explicit, there by completely avoids the problems associated with simultaneity in this method scale as  $N_r$ ,  $N_r$  being the number of real space discretization points. The method further imposes no restriction on the type of sources used are not plane wave, but from quantum dot point source to Gaussian beams. More important is the fact that by using FDTD method, we are able to account for the finiteness of the structure in all 3-D. Moreover, the method allows for the explicit examination of the time development of EM waves in the structure and therefore is the best suited algorithm for investigating wave guiding mechanisms and cavity coupling.



However, there are some rather serious drawbacks to this method. For example to calculate the transmission and reflection coefficient, a Gaussian frequency pulse is launched into the plane perpendicular to the pointing vector perpendicular to the corresponding value of a reference medium to yield the transmission and reflection coefficients. This is more tedious and sensitive to errors than the Transfer Matrix Method.

## References

### 1. Basic FDTD readings

- [1] Yee, K. S., "Numerical solution of initial boundary value problems involving Maxwell's equations in isotropic media," *IEEE Transactions on Antennas and Propagation*, 302-307, (1966).
- [2] J. D. Joannopoulos, R. D. Meade and J. N. Winn, *Photonic Crystals—Molding the Flow of Light*, (Princeton University Press, 1995).
- [3] K. Sakoda, *Optical Properties of Photonic Crystals*, (Springer-Verlag, 2001).
- [4] Chu, S. T., Chaudhuri, S.K., "A finite-difference time-domain method for the design and analysis of guided-wave optical structures," *Journal of Lightwave Technology*, 2033-2038, (1989).
- [5] Taflove, A., Hagness, S., "Computational Electrodynamics: The Finite-Difference Time-Domain Method," Second edition, Artech House, Boston, (2000).

### 2. Material models

- [6] Ziolkowski, R. W., "Incorporation of microscopic material models into FDTD approach for ultrafast optical propagation," *IEEE Transactions on Antennas and Propagation*, 375-391, (1997).
- [7] Liang, T., Ziolkowski, R. W., "Dispersion effects on grating-assisted output couplers under ultra-fast pulse excitations", *Microwave and Opt. Tech. Lett.*, **17**, 17-23, (1998).

### 3. Perfectly Matched Layer (PML) boundary conditions

- [8] Bérenger, J. P., "A perfectly matched layer for the absorption of electromagnetic waves," *Journal of Computational Physics*, **114**, 185-200, (1994). Gedney, S. D., "An anisotropic perfectly matched layer absorbing media for the truncation of FDTD lattices," *IEEE Transactions on Antennas and Propagation*, 1630-1639, (1996).
- [9] Taflove, A., "Advances in Computational Electrodynamics — The Finite-Difference Time-Domain Method", Artech House, Boston, Ch. 5, (1998).